Published OnlineFirst August 17, 2012; DOI: 10.1158/0008-5472.CAN-12-1727

Cancer Research

A Retinoic Acid–Rich Tumor Microenvironment Provides Clonal Survival Cues for Tumor-Specific CD8 + T Cells

Yanxia Guo, Karina Pino-Lagos, Cory A. Ahonen, et al.

Cancer Res 2012;72:5230-5239. Published OnlineFirst August 17, 2012.

Published OnlineFirst August 17, 2012; DOI: 10.1158/0008-5472.CAN-12-1727

A Retinoic Acid—Rich Tumor Microenvironment Provides Clonal Survival Cues for Tumor-Specific CD8$^+$ T Cells

Yanxia Guo[1], Karina Pino-Lagos[1], Cory A. Ahonen[1], Kathy A. Bennett[1], Jinshan Wang[3], Joseph L. Napoli[3], Rune Blomhoff[5], Shanthini Sockanathan[6], Roshantha A. Chandraratna[4], Ethan Dmitrovsky[2], Mary Jo Turk[1], and Randolph J. Noelle[1,7]

Abstract

While vitamin A has been implicated in host resistance to infectious disease, little is known about the role of vitamin A and its active metabolite, retinoic acid (RA) in host defenses against cancer. Here, we show that local RA production within the tumor microenvironment (TME) is increased up to 5-fold as compared with naïve surrounding tissue, with a commensurate increase in RA signaling to regionally infiltrating tumor-reactive T cells. Conditional disruption of RA signaling in CD8$^+$ T cells using a dominant negative retinoic acid receptor α (dnRARα) established that RA signaling is required for tumor-specific CD8$^+$ T-cell expansion/accumulation and protective antitumor immunity. *In vivo* analysis of antigen-specific CD8$^+$ T-cell responses revealed that early T-cell expansion was RA-independent; however, late T-cell expansion and clonal accumulation was suppressed strongly in the absence of RA signaling. Our findings indicate that RA function is essential for the survival of tumor-reactive CD8$^+$ T cells within the TME. *Cancer Res; 72(20); 5230–9. ©2012 AACR.*

Introduction

The morphogenic role of the active form of vitamin A, retinoic acid (RA), in controlling spatial and temporal developmental patterning has underscored the powerful and essential function of this mediator during embryogenesis (1, 2). Similarly, within the immune system, RA has been shown to exert profound effects as a differentiation factor in inducing gut homing of leukocytes (3–6), the differentiation and stability of adaptive regulatory T cells (7–9), the differentiation of CD4$^+$ T cells toward T-helper 1(T_H1)/T_H17 cells (10, 11), IgA class switching in B cells (6), and the differentiation of myeloid cells (12, 13). It has been proposed that regionalized production of RA is critical for its role as an immune differentiation factor (11). Genetic approaches of ablating RA signaling in T cells have established how RA influences CD4$^+$ T-cell response *in vivo* (10, 11), but little is known about its role in governing CD8$^+$ T-cell responsiveness. Given the well-recognized role of RA in supporting T-cell responses, and the need for robust T-cell responses in the development of protective antitumor immunity (14), the role of RA in the host resistance against cancer was addressed with a focus on CD8$^+$ T-cell expansion and function. The studies presented herein show that RA is abundantly produced within the tumor microenvironment (TME) and accumulates to levels much higher than in surrounding tissue. Selective disruption of RA signaling in CD8$^+$ T cells incapacitates their ability to undergo effective clonal expansion *in vivo* and as such, interferes with the development of protective antitumor immunity.

Authors' Affiliations: [1]Department of Microbiology and Immunology, The Geisel School of Medicine at Dartmouth, Norris Cotton Cancer Center, Lebanon, New Hampshire; [2]Department of Pharmacology and Toxicology, The Geisel School of Medicine at Dartmouth, Hanover, New Hampshire; [3]Program in Metabolic Biology, Nutritional Science and Toxicology, University of California-Berkeley, Berkeley; [4]IO Therapeutics, Santa Ana, California; [5]Department of Nutrition, Institute of Basic Medical Sciences, University of Oslo, Oslo, Norway; [6]The Solomon H. Snyder Department of Neuroscience, Johns Hopkins University School of Medicine, Baltimore, Maryland; and [7]Medical Research Council Centre of Transplantation, Guy's Hospital, King's College London, King's Health Partners, London, United Kingdom

Note: Supplementary data for this article are available at Cancer Research Online (http://cancerres.aacrjournals.org/).

Corresponding Author: Randolph J. Noelle, Norris Cotton Cancer Center, One Medical Center Drive, Rubin Bldg., Room 730, Lebanon, NH 03755. Phone: 603-653-9908; Fax: 603-653-9952; E-mail: Randolph.J.Noelle@Dartmouth.edu

doi: 10.1158/0008-5472.CAN-12-1727

Materials and Methods

Animals

C57BL/6 (CD45.1) and C57BL/6 (CD45.2) were purchased from National Cancer Institute (Bethesda, MD). CD4^{Cre} and OTI transgenic mice were from Jackson Laboratory. The DR5-Luciferase (4) and dominant negative retinoic acid receptor α (dnRARα) mice (15) are as previously described. All animals were maintained in a pathogen-free facility at Geisel School of Medicine at Dartmouth (Hanover, NH).

Tumor

B16.Ovalbumin (B16.OVA) melanoma cell line was generated (16) by overexpressing chicken OVA-RFP in B16-F10 (obtained from Mary Jo Turk in 2005). B16.OVA was transduced with plasmid containing DR5-Luciferase to generate B16.OVA-DR5-Luciferase cell line. Both cell lines were periodically authenticated by morphologic inspection and tested negative for *Mycoplasma* contamination by PCR tests in 2008 to 2012, and last time tested in February 2012. For tumor growth curve measurement, 0.5×10^5 B16.OVA cells were injected into mice intradermally and measured 3 times a week.

Published OnlineFirst August 17, 2012; DOI: 10.1158/0008-5472.CAN-12-1727

For whole body imaging (WBI), OVA-tetramer staining and IFN-γ enzyme-linked immunosorbent spot (ELISPOT) assay, 1.5×10^5 B16.OVA cells were injected. To deplete $CD4^+$ T cells, mice received 250 μg αCD4 (clone GK1.5, BioXcell). For pan-RAR antagonist treatment, recipient mice were treated intraperitoneally (i.p.) 3 times per week with control vehicle [dimethyl sulfoxide (DMSO)] or 25 μg/mouse Pan-RAR antagonist (NRX 194310, NuRX Pharmaceuticals).

Monoclonal antibodies

The following FITC-, PE-, PerCP-, APC-Cy7-, Pacific Blue- or APC-conjugated antibodies were used: α-CD45.1 (A20), α-CD45.2 (104), α-CD8 (53–6.7), α-CD11c (N418), α-CD62L (Mel-14), α-CD11b (M1/70), α-CD44 (IM7), α-MHCII (M5), α-IFN-γ (XMG1.2), α-CD69 (H1.2F3), α-BrdUrd (PRB-1), and α-α4β7 (DATK32). All antibodies were purchased from BioLegend except α-BrdUrd and anti-α4β7 (BD Biosciences). MitoTracker Green was purchased from Invitrogen. 7-AAD (BD Biosciences) or LIVE/DEAD Fixable Near-IR Dead Cell Stain Kit (Invitrogen) was used to exclude dead cells in fluorescence-activated cell sorting (FACS) analysis.

Imaging and luciferase assay

WBI and luciferase activity of purified cells (5×10^5 cells per well) was conducted as previously described (11). For *in vitro* cultured B16.OVA-DR5-Luciferase tumor cells, cells were cultured for 24 hours with RA and Pan-RAR antagonist (2.5 μg/mL), plated at 1×10^6 cells per well, administrated D-luciferin at 150 μg/mL, and imaged. Analysis and images were obtained using the Living Image Software (version 2.6.1).

All-trans retinoic acid measurement

Tumor, tumor-draining lymph node (TDLN), and spleen were taken from day 6 B16.OVA-bearing or naïve mice. Liquid chromatography/tandem mass spectrometry (LC/MS-MS) was used as described previously to measure all-trans retinoic acid (ATRA) concentration (17).

RALDH activity analysis

RALDH activity in individual cells was estimated using ALDEFLUOR staining kits (StemCell Technologies), according to the manufacturer's protocol as previously described (18). For immunophenotyping of $ALDH^{bri}$ cells, the cells were subsequently stained with PE-, PerCP-, APC-, PE-Cy7-, or APC-Cy7–conjugated monoclonal antibody (mAb) in ice-cold ALDEFLUOR assay buffer. Cells were analyzed using FACS Calibur or MACS Quant (Miltenyi Biotech).

Bone marrow chimera mice

C57BL/6 (CD45.1) or DR5-Luciferase (CD45.2) mice were lethally irradiated and received 5×10^6 bone marrow cells harvested from DR5-Luciferase and C57BL/6 (CD45.1), respectively. Reconstitution was confirmed 8 weeks later by staining with α-CD45.1 and α-CD45.2. All BMCs exceeded 96% reconstitution efficiency.

Immunization

dnRARα and dnRARα$CD4^{Cre}$ mice were immunized with 500 μg Ovalbumin (Sigma–Aldrich), 50 μg αCD40 (BioXcell), and 50 μg polyI:C (InvivoGen) by intraperitoneal injection.

Analysis of MHC-I tetramer and IFN-γ by flow cytometery

MHCI-I tetramer and IFN-γ staining was conducted as previously described (19). Four-color FACS data were collected on a BD FACSCalibur flow cytometer and analyzed using FlowJo software. Analysis typically pregated on $CD8^+MHCII^-$ cells.

ELISPOT assay

ELISPOT was done according to the procedures described previously (20). Briefly, $CD8^+$ effector T cells were harvested from spleen, TDLN, or tumor-infiltrating lymphocytes (TIL) of day 12 B16.OVA-bearing mice, and plated at 1:1 ratio with irradiated T-cell–depleted C57BL/6 splenocytes pulsed with 10 μg/mL SIINFEKL peptide (or without peptide as control). Plates were incubated for 20 hours at 37°C and then developed with aminoethylcarbazole chromogen.

Phenotype analysis of OVA-specific $CD8^+$ T cells

Enrichment was done at different time points as described previously (21) and stained as described in the text.

Statistical analysis

Data graphs were made using GraphPad Prism software and expressed as the mean ± SEM or mean ± SD. Differences for graphs with one grouping variables were analyzed by Student *t* test (2 groups). For studies of B16.OVA tumor growth and OVA tetramer kinetics, 2-way ANOVA was used to assess significance. In all analysis, *, $P < 0.05$; **, $P < 0.01$; ***, $P < 0.001$, and ns denotes $P > 0.05$.

Results

Heightened RA signaling and RA synthesis within the TME

We previously reported that inflammatory mediators induced a spatially and temporally restricted induction of RA synthesis and signaling *in vivo* (11). To determine if tumor growth *in vivo* induced restricted and heightened RA signaling and synthesis, a tumor that reports RA signaling was injected *in vivo*. During the growth of B16.OVA-DR5-Luciferase, in which the RA response element, DR5 repeat, is coupled to a luciferase reporter, an increase of RA signaling over the tumor growth course (Fig. 1A) was observed. The reporting signal was RA-dependent, as it was inhibited by the administration of pan-RAR antagonist (NRX 194310; data not shown). The same RA reporting signal was also observed using B16-DR5-Luciferase cells, indicating that expression of OVA was not critical for induction of RA (data not shown). To confirm that enhanced RA synthesis at the tumor site was induced during tumor growth, DR5-Luciferase transgenic reporter mice were used, which express DR5-luciferase in all tissues (4). B16.OVA tumor cells were injected into DR5-Luciferase mice and RA signaling could be readily detected primarily at the growing tumor site by day 6 (Fig. 1B). The induced RA signaling was also observed in other tumor models, such as EL4 thymoma, MB49 urothelial cacrcinoma, and B16 melanoma (data not shown). To

Published OnlineFirst August 17, 2012; DOI: 10.1158/0008-5472.CAN-12-1727

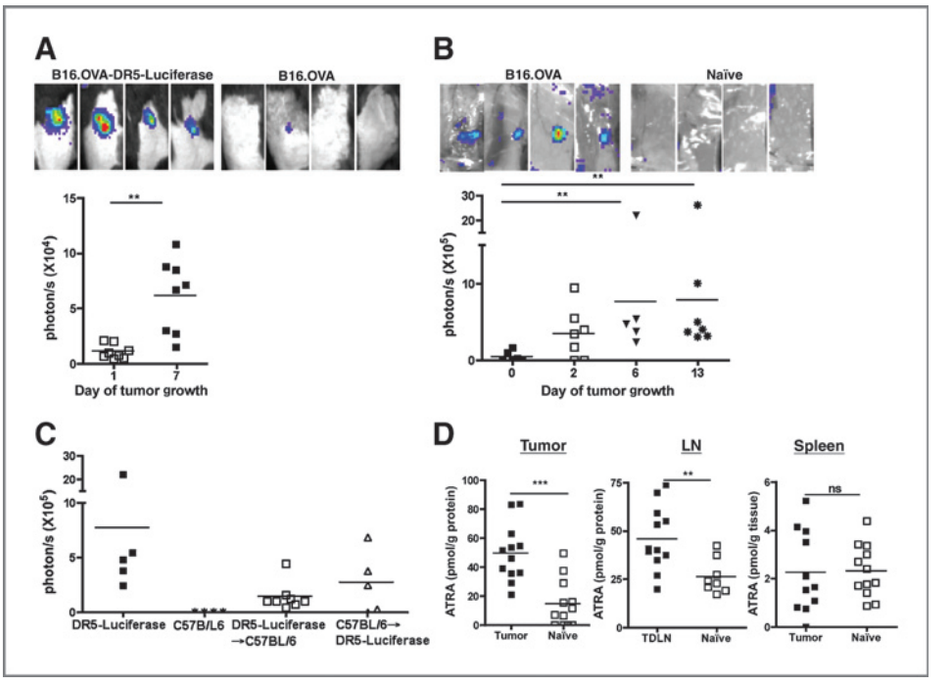

Figure 1. RA signaling is induced at the tumor site in tumor-bearing mice. A, WBI of RA signaling by B16.OVA-DR5-Luciferase tumor cells. Representative tumor sites of B16.OVA-DR5-Luciferase (left) and B16.OVA (right) in C57BL/6 mice on day 6 by WBI are shown. Quantification of RA reporting signals at the tumor site is shown on bottom on day 1 and 7 posttumor inoculation. Data presented are representative of 4 experiments with similar imaging patterns. B, WBI of RA signaling in DR5-Luciferase mice. Representative tumor sites of day 6 B16.OVA-bearing (left) and naïve (right) DR5-Luciferase mice (top) by WBI are shown. Kinetics of quantified RA signaling at the tumor site is shown at the bottom. This represents quantified WBI of mice ($n = 3$–4 mice per experiment) pooled from 2 experiments. C, impact of the hematopoietic and nonhematopoietic compartments in tumor-induced RA reporting. Quantification of total photon flux at tumor sites from B16.OVA-bearing DR5-Luciferase, C57BL/6, DR5-Luciferase→C57BL/6 BMC, and C57BL/6→/DR5-Luciferase BMC mice on day 6 after tumor administration. Data shown are pooled from 2 separate experiments. D, analysis of ATRA concentrations in tumor-bearing mice. B16.OVA cells were inoculated as in A–C. Tumor tissue, TDLN, and spleen from tumor-bearing and naïve mice were collected on day 6 and ATRA concentration was measured. Each value represents the same tissue pooled from 4 mice. Data shown are pooled from 2 experiments. In all experiments shown here, statistically significant differences were determined by *t* test.

distinguish RA signaling in hematopoietic cells and/or nonhematopoietic compartment in the TME, bone marrow chimeras (BMC) were generated (designated as donor bone marrow → lethally irradiated recipient): DR5-Luciferase→C57BL/6 and C57BL/6 → DR5-Luciferase. Local RA responses in the TME were observed in both recipients as nonreconstituted mice, indicating RA signaling in both hematopoietic and nonhematopoietic cells (Fig. 1C).

To directly measure RA synthesis within the TME, ATRA concentrations from TDLN, spleen, and tumor site were quantified by LC/MS-MS. Data showed that ATRA was significantly increased (~5-fold) in tumor tissue as compared with naïve skin (Fig. 1D). The same trend was also true when ATRA quantity in TDLN was compared with that in naïve lymph node (LN; ~2-fold increase). Conversely, no significant difference was observed in the ATRA levels between spleen from naïve mice and B16.OVA-bearing mice. Taken together, these results showed that RA synthesis and signaling is elicited locally in response to tumor growth *in vivo*.

The host, but not the tumor, produces RA to enhance RA concentration in the TME

A series of studies were designed to determine the relative contribution of the host and tumor cells to elevated levels of RA in the TME. First, real-time (RT-PCR) analysis for the expression of *Aldh1a1–3* (encoding RALDH1–3, critical enzymes for RA synthesis) in B16.OVA cells compared with the expression in granulocyte macrophage colony-stimulating factor (GM-CSF) or RA-stimulated dendritic cells (DC; ref. 18) showed (Fig. 2A) that B16.OVA cells expressed no detectable *Aldh1a1* or *Aldh1a2*, and expressed very low *Aldh1a3*. Second, luciferase activity measured in B16.OVA-DR5-Luciferase cells *in vitro* was only detectable if exogenous RA (as little as 1nM RA) was added, indicating that the cells produce little if any RA that can drive reporter activity (Fig. 2B). This reporting signal was RA-dependent, as evidenced by its inhibition by Pan-RAR antagonist. Third, RA synthesis *in vivo* by tumor cells was assessed by ALDEFLOUR (ALDH) staining. As can be seen (Fig. 2C), *ex vivo* analysis of the $CD45^{-}RFP^{+}$ cells (tumor) did not report as $ALDH^{bri}$ [0.053% −DEAB (diethylaminobenzaldehyde) vs. 0.047% +DEAB], whereas the $CD45^{+}RFP^{-}$ cells in the tumor site were $ALDH^{bri}$ (0.11% −DEAB vs. 0.013% +DEAB). Taken together, tumor cells contribute little, if at all, directly to elevated tissue levels of ATRA.

Attention was turned to identifying host cells producing elevated levels of ATRA within the TME. RA is constitutively produced in naïve skin (Fig. 2D, top) as reported previously (22). However, on day 5 posttumor inoculation, there was a significant increase in $ALDH^{bri}$% within the TME as compared

Published OnlineFirst August 17, 2012; DOI: 10.1158/0008-5472.CAN-12-1727

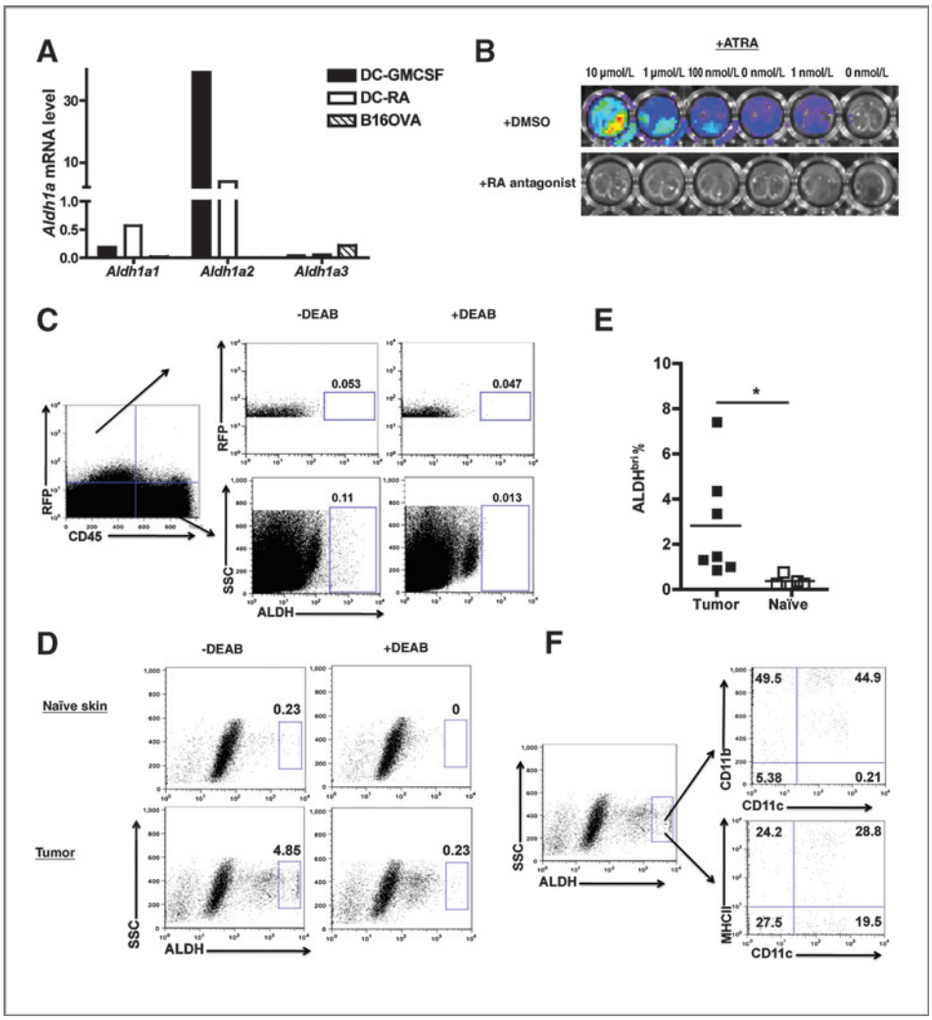

Figure 2. Analysis of the cellular source of RA in tumor-bearing mice. A, RT-PCR analysis of *Aldh1a1*, *Aldh1a2*, and *Aldh1a3* expression in DCs and tumor cells. GM-CSF or RA-treated CD11c$^+$ DCs and *in vitro* cultured B16.OVA tumor cells were analyzed for mRNA expression of *Aldh1a1*, *Aldh1a2*, and *Aldh1a3*. This is representative of 2 experiments. B, lack of constitutive RA reporting in B16.OVA-DR5-Luciferase tumor cells. Representative *in vitro* imaging of control or RA-treated B16.OVA-DR5-Luciferase cells. RA was used at indicated concentration in culture in the presence of vehicle control (DMSO; top) or Pan-RAR antagonist (bottom). This is representative of 3 experiments with similar results. C, *ex vivo* analysis of tumor RALDH activity. Skin tissues from naïve mice and tumor tissues of day 5 tumor-bearing mice were analyzed for RALDH activity. Data shown are gated on live cells, and RALDH activity is resolved in the RFP$^+$ CD45$^-$ (tumor) and RFP$^-$CD45$^+$ hematopoietic (immune) populations. D, *ex vivo* analysis of TILs within the TME for expression of RALDH activity. The samples were prepared as in C, but shown data gated on total live cells with tumor cells excluded. E, quantified ALDH^{bri} population in TILs. The frequency of ALDH^{bri} among total live TILs or naïve skin-residential cells was determined. F, phenotypic analysis of ALDH^{bri} populations in TILs. Data shown in C–F are representative of 3 independent experiments with similar results ($n \geq 3$ mice per group), and data shown in (E) are pooled from 2 experiments ($n = 6$–7 mice per group). Statistically significant differences were determined by *t* test. SSC, side scatter.

with the naïve skin (Fig. 2E, 2.83% ± 0.91% vs. 0.36% ± 0.09%, $P < 0.05$). The frequency of ALDH^{bri} cells increased as the tumor grows, showed by higher ALDH^{bri}% of TILs on day 14 and 22 than day 5 of tumor growth (data not shown). Further analysis showed that the ALDH^{bri} cells comprises various DCs and macrophage subsets, including CD11c$^+$CD11b^{hi}, CD11c$^+$ CD11b$^-$ DCs, and CD11c$^-$CD11b$^+$ macrophages (Fig. 2F). Analysis indicated that approximately 50% of ALDH^{bri} cells express high levels of MHCII (Fig. 2F), indicating they may be mature antigen-presenting cells (APC) within the TME. Taken together, the data suggest that the tumor-infiltrating DCs and macrophages contribute to RA-enriched TME.

RA signaling occurs in CD8$^+$ T cells within the TME and TDLN

Further studies were designed to determine the lineage of cells being signaled by RA within the TME and TDLN. To identify the hematopoietic cells reporting RA signaling, specific cell lineages were purified from TIL, TDLN (inguinal LN), and spleen of the DR5-Luciferase mice, and whole-cell luciferase assays were conducted. There were no significant differences between the basal level of luciferase activity in cells from naïve DR5-Luciferase (Luc$^+$) and control mice (Luc$^-$; data not shown). B16.OVA growth induced about approximately 6-fold increase in luciferase activity in CD8$^+$ T cells from the TME in

Published OnlineFirst August 17, 2012; DOI: 10.1158/0008-5472.CAN-12-1727

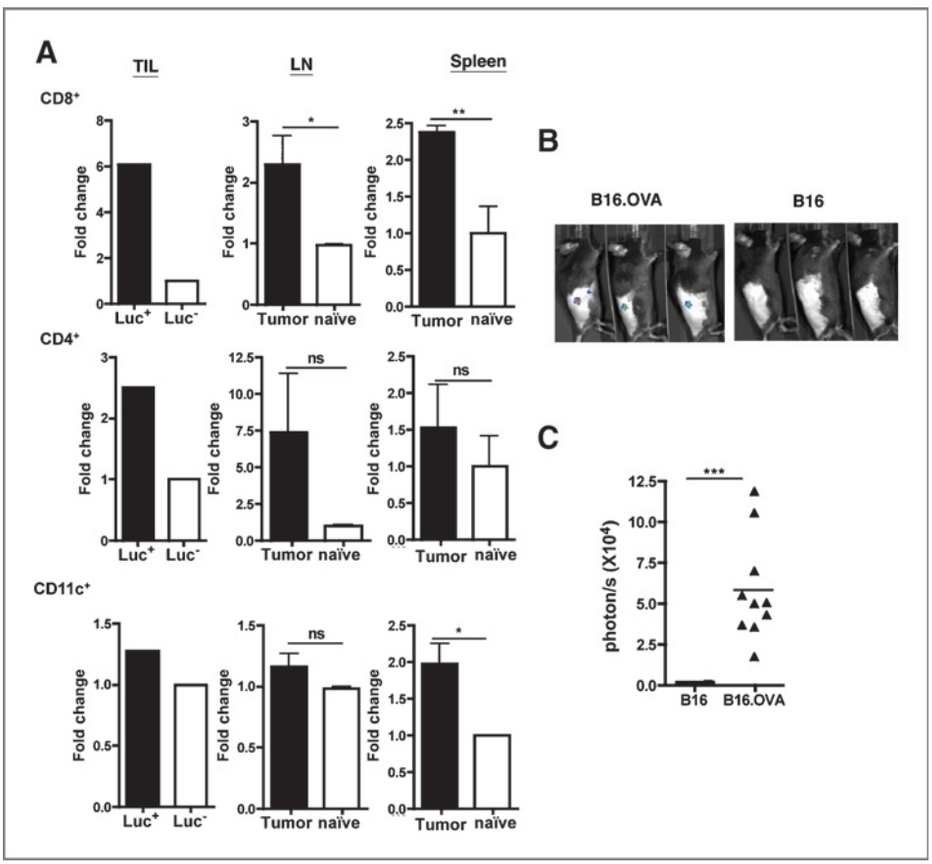

Figure 3. Enhanced RA signaling in T cells in tumor-bearing mice. A, comparative RA signaling in $CD8^+$ T cells, $CD4^+$ T cells, and $CD11c^+$ DCs in tumor-bearing and naïve mice. On day 6 posttumor inoculation, $CD8^+$ T cells, $CD4^+$ T cells, and $CD11c^+$ DCs were isolated from tumor tissue (TIL) of B16.OVA-bearing DR5-Luciferase (Luc^+) or littermate control (Luc^-), TDLN and spleen of B16.OVA-bearing or naïve DR5-Luciferase mice (pooled $\geq$7 mice per group), and total cellular luciferase activity was measured using 5×10^5 cells per well. Bar graphs for TILs show single well without error bars. About LN and spleen, bar graphs show triplicate wells with mean $\pm$ SD. Data shown are representative of 2 experiments with similar results. B, heightened RA reporting of tumor-specific T cells in the TME of tumor-bearing mice. Representative imaging of tumor site of day 6 B16.OVA-bearing C57BL/6 mice receiving adoptive transfer of $CD8^+$ T cells from OTI^{Luc} mice. C, quantified RA reporting of $CD8^+$ TIL. WBI was used to quantify the total photon flux of infiltrating OTI^{Luc} T cells of the RA reporting signal at the tumor site as shown in (B). Shown is pooled data from 2 experiments with total $n \geq 11$ mice per group. In A and C, statistically significant differences were determined by *t* test.

DR5-Luciferase mice (Fig. 3A; TIL Luc^+ vs. Luc^-). However, when the luciferase activity was measured in the same number of cells, there was only approximately 2.5- and 1.2-fold increase in $CD4^+$ T cells and $CD11c^+$ DCs from TME (TIL Luc^+ vs. Luc^-), respectively. The same trend was observed in TDLN and spleen, except that there was also a significant increase in RA signaling in $CD11c^+$ DCs from the spleen (tumor vs. naïve). Thus, $CD8^+$ T cells in the TME showed a marked response to elevated concentrations of ATRA *in vivo*.

To measure tumor-specific $CD8^+$ T-cell response to heightened RA concentration in the TME, naive OVA-specific $CD8^+$ T cells from DR5-Luciferase $\times$ OTI (OTI^{Luc}) mice were transferred into B16 and B16.OVA-bearing mice, respectively. $CD8^+$ T cells in OTI^{Luc} mice recognize OVA antigen and elicit luciferase activity when RA signaling occurs. As shown in Fig. 3B and C, in B16.OVA-bearing mice, OTI^{Luc} T cells showed robust RA response signal at the tumor site as compared with nondetectable RA reporting signals in B16-bearing mice. This further confirmed that $CD8^+$ T cells are responsive to RA produced at the tumor site in a tumor-specific manner.

Disruption of RA signaling in $CD8^+$ T cells *in vivo* impairs antitumor response

High ATRA tissue levels and RA signaling induced at the tumor site suggests that RA may be important in regulating tumor-specific immunity. To address the functional importance of RA signaling to $CD8^+$ T-cell function, a dominant negative $RAR\alpha^{403}$ (dnRARα; ref. 15) was overexpressed in T cells by interbreeding the dnRARα with $CD4^{Cre}$ mice. Studies showed that dnRARα$CD4^{Cre}$ mice expressed Cre-dependent dnRARα in both $CD4^+$ and $CD8^+$ T cells (Supplementary Fig. S1A). In addition, it was confirmed that $CD8^+$ T cells in dnRARα$CD4^{Cre}$ were unresponsive to RA *in vitro*, as shown by the inability to upregulate α4β7 in response to RA (Supplementary Fig. S1B) and that the dnRARα$CD4^{cre}$ did not disrupt signaling through peroxisome proliferator-activated receptor γ and vitamin D receptor (23; data not shown).

Published OnlineFirst August 17, 2012; DOI: 10.1158/0008-5472.CAN-12-1727

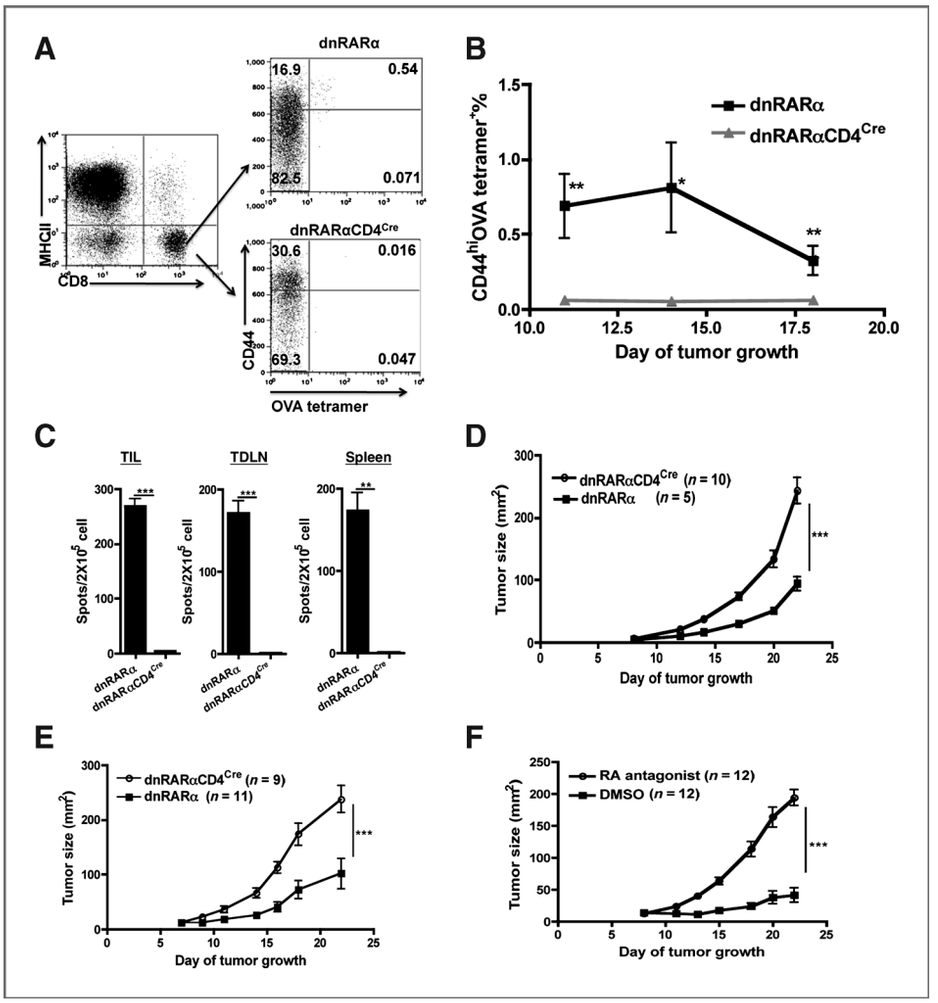

Figure 4. Disruption of RA signaling in CD8$^+$ T cells impairs the antitumor CD8$^+$ T-cell immune response. A–C, impact of RA signaling on the OVA-specific CD8$^+$ T-cell expansion and function in B16.OVA-bearing mice. Mice were injected with 1.5×10^5 B16.OVA cells intradermally on day 0. CD4$^+$ T cells were depleted on day −2, 4, and 10. Mice were bled on day 11, 14, and 18 for OVA-tetramer staining. Representative FACS analysis of the frequency of blood OVA-tetramer$^+$ CD8$^+$ T cells in B16.OVA-bearing dnRARα and dnRARαCD4^{Cre} mice, respectively, was determined (A and B). Data presented are pooled from 2 experiments with ($n \geq 14$ mice per group). Error bars indicated SEM. C, decreased IFN-γ production by CD8$^+$ T cells in dnRARαCD4^{Cre} mice. An IFN-γ ELISPOT was conducted with CD8$^+$ T cells purified from TIL, TDLN, and spleen of tumor-bearing dnRARα and dnRARαCD4^{Cre} mice (pooled $n \geq 9$ mice per group) on day 12 posttumor inoculation. Bar graphs show triplicate wells with errors bars depicting ± SD. Data are representative of 2 experiments with similar results. Statistically significant differences in B and C were determined by *t* test. D and E, enhanced tumor growth in the absence of RA signaling to T cells. B16.OVA cells were injected into dnRARα and dnRARαCD4^{Cre} mice as in A, and growth was monitored over the course of 23 days. Data shown are representative of 4 experiments with similar results ($n \geq 5$ mice per group in each experiment). In one group of experiments (E), CD4$^+$ T cells were depleted as in A. Data presented are representative of 3 experiments ($n \geq 9$ mice per group in each experiment) with similar results. F, an RA antagonist enhances tumor growth *in vivo*. RA antagonist or DMSO control was administrated into C57BL/6 mice every other day from day −1 at 25 μg/mouse by intraperitoneal injection. CD4$^+$ T cells were depleted as in A and tumor growth was monitored. This is representative of 2 experiments with similar results ($n \geq 10$ mice per group). Statistically significant differences in D–F were determined by 2-way ANOVA analysis with error bars indicating SEM.

With specificity of the dnRARα for RA signaling confirmed, the role of RA signaling on tumor-specific CD8$^+$ T-cell function *in vivo* was evaluated. The endogenous OVA-specific CD8$^+$ T-cell response in B16.OVA-bearing dnRARαCD4^{Cre} and dnRARα mice was measured. As previously published in B16 melanoma model (24), CD4$^+$ T-cell depletion induces greater endogenous CD8$^+$ T-cell priming against tumor-associated antigen in B16.OVA model. Therefore, to measure more robust CD8$^+$ T-cell response in the absence of CD4$^+$ T cells and irrefutably assign any functional impact of RA signaling disruption to CD8$^+$ T cells, B16.OVA were injected into CD4$^+$ T cell-depleted dnRARα and dnRARαCD4^{Cre} mice. Ablation of RA signaling in the dnRARαCD4^{Cre} mice resulted in a marked decrease of CD44^{hi}OVA-tetramer$^+$ CD8$^+$ T cells as compared with the equivalent cells in the control mice over the tumor growth course (Fig. 4A and B). Furthermore, there was a significant decrease in IFN-γ–producing CD8$^+$ T cells from tumor tissue (TIL 4.3 ± 0.67 vs. 269.0 ± 12.9, $P < 0.001$), TDLN (1.0 ± 0.57 vs.171 ± 15.1, $P < 0.001$), and spleen (0.66 ± 0.33 vs. 173.37 ± 21.37, $P < 0.01$) in dnRARαCD4^{Cre} as compared with

Published OnlineFirst August 17, 2012; DOI: 10.1158/0008-5472.CAN-12-1727

dnRARα mice (Fig. 4C), respectively. The fewer functional OVA-specific $CD8^+$ T cells in dnRARαCD4^{Cre} mice suggests that RA signaling is required for tumor-specific $CD8^+$ T-cell accumulation and function in the TME.

Faster B16.OVA growth was observed in dnRARαCD4^{Cre} mice in comparison with dnRARα mice (Fig. 4D), suggesting reduced immune surveillance. The enhanced tumor growth was independent of deficient $CD4^+$ T cell help because the same effect was observed when $CD4^+$ T cells were depleted in both groups over the entire tumor growth course (Fig. 4E). Chemical inhibition of RA signaling recapitulated the phenotype observed in the dnRARαCD4^{Cre} mice (Fig. 4F). *In vitro* culture experiments established that the pan-RAR antagonist used in this study did not inhibit B16.OVA growth over a wide dose range (data not shown). In conclusion, these studies establish that RA signaling to $CD8^+$ T cells *in vivo* is critical for optimal suppression of tumor growth.

RA signaling is required for $CD8^+$ T-cell expansion *in vivo*

To gain greater insights into the underlying mechanism of RA controlling $CD8^+$ T-cell clonal expansion, a more robust $CD8^+$ T-cell response induced by CD40 agonist, together with a TLR agonist and soluble antigen system was exploited (19). As observed in the B16.OVA tumor model, dnRARαCD4^{Cre} mice showed a significant decrease in the frequency of OVA-specific $CD8^+$ T cells as compared with control dnRARα mice (14.9% vs. 0.6%; Fig. 5A and B). CD44^{hi}OVA-tetramer$^+$ $CD8^+$ T cells were quantified in the blood, spleen, mesenteric LN (MLN), and peripheral LN (PLN) on peak response time of day 6 to ensure that the reduced frequency in the blood was not due to a

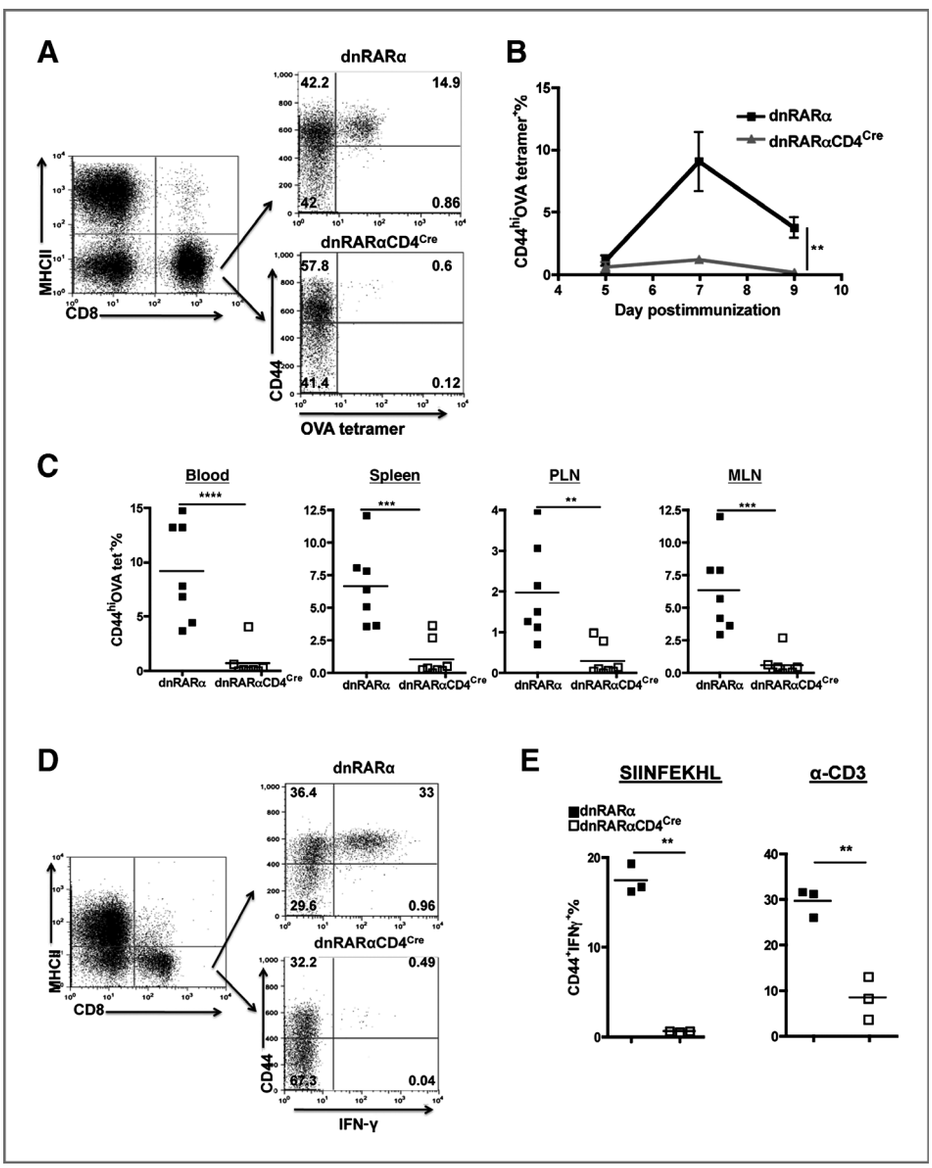

Figure 5. Disruption of RA signaling in $CD8^+$ T cells impairs clonal expansion and function *in vivo* in response to OVA, α-CD40, and pI:C immunization. dnRARα and dnRARαCD4^{Cre} mice were immunized as described in Material and Methods on day 0. A–C, reduced clonal expansion. Representative analysis of tetramer staining (A), kinetics in the blood (B), and distribution of OVA tetramer$^+$ cells in blood, spleen, PLN, and MLN (day 6; C) are shown. In all the examined organs, shown is the CD44^{hi}OVA tetramer$^+$ percentage in $CD8^+$MHCII$^-$ T cells. Data shown in A and B are representative of 4 experiments ($n \geq 3$ mice per group in each experiment). Statistically significant differences were determined by 2-way ANOVA analysis of pooled experiments ($n \geq 12$ mice per group) in B. Data shown in C are pooled from 2 experiments ($n = 7$ mice per group). Statistically significant differences were determined by *t* test. D and E, reduced IFN-γ recall responses. Blood samples from immunized mice as in A–C (day 6 postimmunization) were incubated in the presence of brefeldin A with or without SIINFEKL peptide or α-CD3 for 18 hours at 37°C. Cytoplasmic IFN-γ staining was determined (D) and quantified (E) and reported as the CD44$^+$IFN-γ$^+$ percentage in $CD8^+$ T cells after restimulation. Statistically significant differences were determined by *t* test. Data shown are representative of 4 experiments with similar results ($n \geq 3$ mice per group in each experiment).

Published OnlineFirst August 17, 2012; DOI: 10.1158/0008-5472.CAN-12-1727

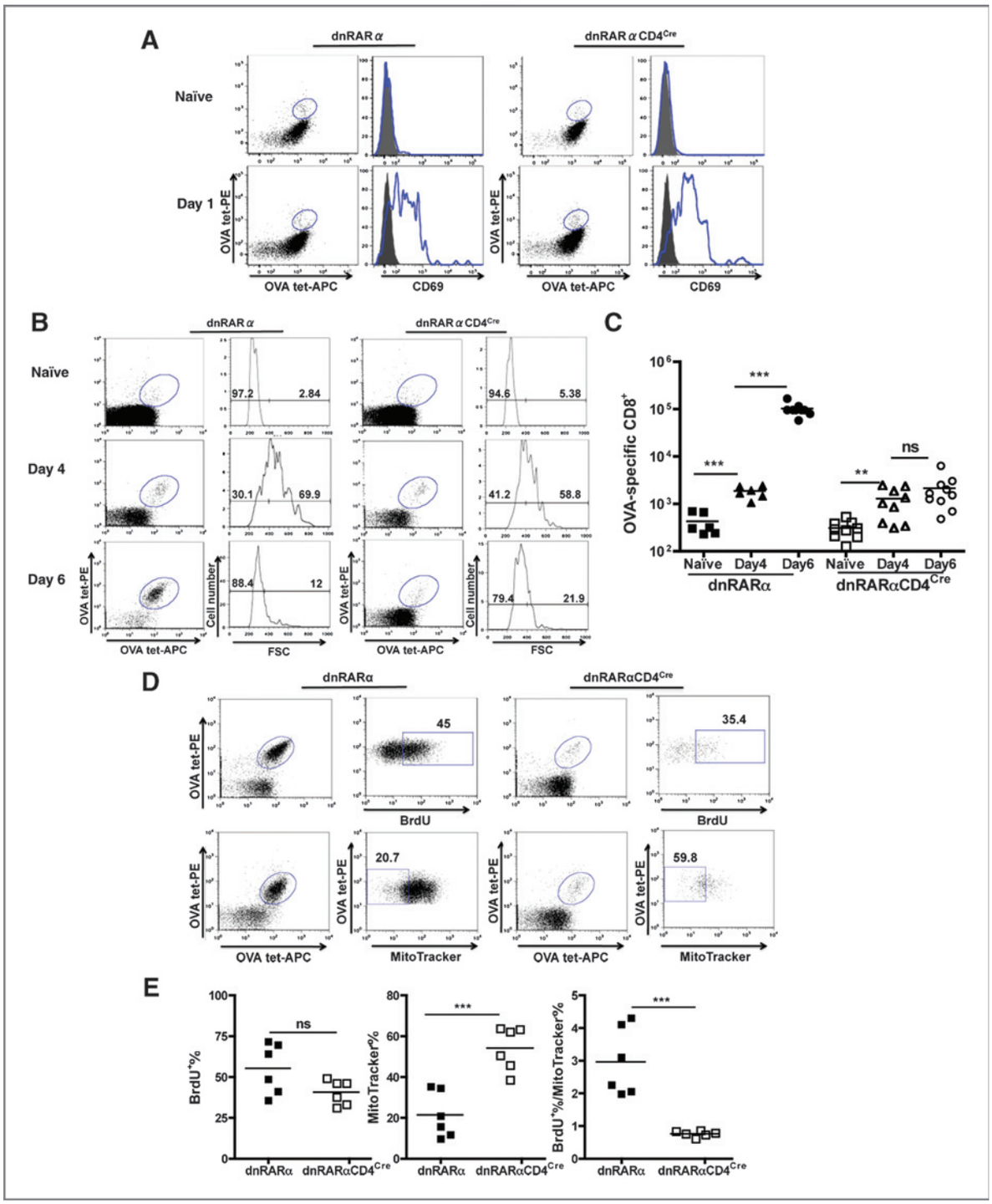

Figure 6. RA signaling is required for CD8$^+$ T-cell accumulation. OVA-specific CD8$^+$ T cells were enriched as described previously. A, CD69 expression on OVA-specific CD8$^+$ T cells on day 1 postimmunization. Mice were immunized and analyzed on day 0 (naïve) and day 1. CD69 is shown on the right next to the enriched OVA-specific CD8$^+$ T cells. B, OVA-tetramer$^+$ T cells from dnRARα and dnRARαCD4^{Cre} blast in response to antigen *in vivo*. Representative FACS plots showing enriched OVA-specific CD8$^+$ T cells on day 0 (top plots), 4 (center plots), and 6 (bottom plots) postimmunization in dnRARα (left) and dnRARαCD4^{Cre} (right) mice, respectively. Forward scatter (FSC) is shown in each group on the right next to the enriched CD8$^+$ T-cell plots. Data in A and B are representative of 2 experiments. C, quantification of OVA-tetramer$^+$ CD8$^+$ T cells over time. Total OVA-specific CD8$^+$ T cells were quantified in naïve, day 4 or 6-immunized dnRARα and dnRARαCD4^{Cre} mice, respectively. Data are pooled from 2 experiments, with $n \geq 6$ mice per group. D, BrdUrd incorporation (top) and MitoTracker staining (bottom) in OVA-Tetramer$^+$ CD8$^+$ T cells upon immunization. BrdUrd was injected i.p. into mice on day 4 and 5 postimmunization. Mice were analyzed on day 6. About MitoTracker staining, mice were analyzed on day 5. E, quantification of BrdUrd and apoptosis in OVA-Tetramer$^+$ CD8$^+$ T cells upon immunization. Quantification of BrdUrd$^+$ (day 6) and MitoTracker$^-$ (day 5) OVA-specific CD8$^+$ T cells. Shown data are pooled from 2 experiments with $n = 6$ mice per group. All statistically significant differences were determined by *t* test. All shown FACS plot is pregated on CD8$^+$MHCII$^-$CD4$^-$CD19$^-$ T cells.

Published OnlineFirst August 17, 2012; DOI: 10.1158/0008-5472.CAN-12-1727

trafficking defect but rather was representative of the overall $CD8^+$ T-cell response (Fig. 5C). When restimulated *ex vivo* by SIINFEKL peptide or α-CD3, the frequency of IFN-γ–producing $CD8^+$ T cells in dnRARα$CD4^{Cre}$ was significantly lower than in dnRARα mice (Fig. 5D and E). Identical results were obtained in mice that were depleted of $CD4^+$ T cells (Supplementary Fig. S2), establishing that intrinsic RA signaling deficiency in $CD8^+$, but not $CD4^+$ T cells, accounted for the defective $CD8^+$ T-cell accumulation.

RA is responsible for the late clonal expansion of $CD8^+$ T cells

Tetramer enrichment allowed for the quantification of total OVA-$tetramer^+$ $CD8^+$ T cells at very early time-points following immunization (21). On day 1 and 4 postimmunization, CD69 expression as well as increases in forward scatter, respectively, of OVA-$tetramer^+$ $CD8^+$ T cells from dnRARα$CD4^{Cre}$ and dnRARα mice were indistinguishable (Fig. 6A and B), indicating that the expression of dnRARα imparts no effect on early T-cell activation. During the initial expansion between day 0 and 4, OVA-$tetramer^+$ $CD8^+$ T cells in dnRARα$CD4^{Cre}$ mice accumulated to the same extent as their counterparts in dnRARα mice, showed by the same approximately 4-fold increase over naïve control (Fig. 6C). However, OVA-specific $CD8^+$ T cells failed to accumulate further between day 4 and 6 in dnRARα$CD4^{Cre}$ mice, whereas the counterparts in dnRARα mice expanded logarithmically (∼50-fold).

Analysis of proliferation of OVA-specific $CD8^+$ T cells by bromodeoxyuridine (BrdUrd) incorporation between day 4 and 6 revealed a slight but not significant decrease in OVA-$tetramer^+$ cells incorporating BrdUrd between dnRARα and dnRARα$CD4^{Cre}$ (both between 40% and 50%; Fig. 6D and E). To determine if there was a survival deficiency of the proliferating $CD8^+$ T cells in dnRARα$CD4^{Cre}$ mice, enriched OVA-specific $CD8^+$ T cells were stained with MitoTracker on day 5 post-immunization. Interestingly, while approximately 20% of the cells were MitoTracker-negative (undergoing apoptosis) in control dnRARα mice, approximately 50% of OVA-$tetramer^+$ $CD8^+$ T cells were MitoTracker-negative in dnRARα$CD4^{Cre}$ mice (Fig. 6D). Therefore, the abortive accumulation of OVA-specific $CD8^+$ T cells in dnRARα$CD4^{Cre}$ mice between day 4 and 6 postimmunization may be due to an equal number of cells undergoing proliferation and apoptosis simultaneously (Fig. 6E). In conclusion, although early $CD8^+$ T-cell expansion is independent of RA signaling *in vivo*, late $CD8^+$ T-cell clonal accumulation requires RA signaling to maintain better survival during proliferation and effector development.

Discussion

Accumulating evidence suggests that heightened tissue levels of RA develop at sites of inflammation (11). In the present study, we reported for the first time that the tumor induces a temporally and spatially restricted production and heightened accumulation of RA within the TME. Host tissue DCs and macrophages instead of tumor cells, were major contributors to high-level ATRA within the TME. The marked $CD8^+$ T-cell responses to regionally produced RA suggested that the host may exploit RA to facilitate the development of $CD8^+$ T-cell–mediated protective antitumor immunity. The functional importance of RA signaling in $CD8^+$ T cells was confirmed by studies in mice in which the RA signaling in T cells was genetically impaired. RA signaling-deficient $CD8^+$ T cells failed to expand/accumulate and produce IFN-γ, thus leading to enhanced B16.OVA tumor growth. These studies support the notion that the expansion, accumulation, and differentiation of tumor-specific $CD8^+$ T cells are dependent on intrinsic RA signaling. An in-depth *in vivo* analysis of OVA-specific $CD8^+$ T cells revealed RA signaling disruption did not impact on upregulation of early activation markers, cell enlargement, or early *in vivo* expansion induced by OVA immunization. The RA signaling-deficient $CD8^+$ T cells proceed through early rounds of division but fail to ultimately accumulate due to dominant apoptosis in the late clonal expansion. As such, RA signaling seems to render these proliferating cells resistant to apoptosis at the effector phase. Because previous studies have suggested that RA signaling may influence IL-2 expression in activated T cells (25, 26), dnRARα$CD4^{cre}$ mice were treated with IL2/aIL2 complex to restore IL-2 levels. However, this did not overcome the deficiency in OVA-specific $CD8^+$ T-cell expansion in immunization model (data not shown). Additional investigative studies on the molecular basis for how intrinsic RA signaling controls $CD8^+$ T-cell survival at the effector phase are underway.

Disclosure of Potential Conflicts of Interest

R. Blomhoff and has an ownership interest (including patents) in Cgene. E. Dmitrovsky has ownership interest (including patents) in a pending patent. R. A. Chandraratna is employed (other than primary affiliation; e.g., consulting) in Io Pharmaceuticals. He is a consultant/advisory board member, holds title of SAB Chair, and has ownership interest (including patents) in Io Pharmaceuticals. No potential conflicts of interest were disclosed by the other authors.

Authors' Contributions

Conception and design: Y. Guo, C.A. Ahonen, E. Dmitrovsky, M.J. Turk, R.J. Noelle

Development of methodology: Y. Guo, K. Pino-Lagos, C.A. Ahonen, J.L. Napoli, R. Blomhoff, R.A. Chandraratna, E. Dmitrovsky, R.J. Noelle

Acquisition of data (provided animals, acquired and managed patients, provided facilities, etc.): Y. Guo, J. Wang, J.L. Napoli, R. Blomhoff, S. Sockanathan, R.J. Noelle

Analysis and interpretation of data (e.g., statistical analysis, biostatistics, computational analysis): Y. Guo, J.L. Napoli, R. Blomhoff, E. Dmitrovsky, R.J. Noelle

Writing, review, and/or revision of the manuscript: Y. Guo, K. Pino-Lagos, E. Dmitrovsky, M.J. Turk, R.J. Noelle

Administrative, technical, or material support (i.e., reporting or organizing data, constructing databases): Y. Guo, K.A. Bennett

Study supervision: R.J. Noelle

Acknowledgments

The authors thank Dr. Pierre Chambon for insightful discussions on data and manuscript preparation, Drs. Edward Usherwood, Victor C. de Vries, and Jose R. Conejo-Garcia for critically reading the manuscript, and Dr. Joshua J. Obar for technical help.

Grant Support

This work was supported by the NIH (AT005382, AI048667, CA062275, and CA120777), the Medical Research Council Centre for Transplantation, the Biomedical Research Council, The Wellcome Trust, and Samuel Waxman Cancer Research Foundation.

The costs of publication of this article were defrayed in part by the payment of page charges. This article must therefore be hereby marked *advertisement* in accordance with 18 U.S.C. Section 1734 solely to indicate this fact.

Received May 1, 2012; revised July 5, 2012; accepted July 24, 2012; published OnlineFirst August 17, 2012.

Published OnlineFirst August 17, 2012; DOI: 10.1158/0008-5472.CAN-12-1727

References

1. Casci T. Functional genomics: an array of bacterial interactions. Nat Rev Genet 2008;9:652.
2. Niederreither K, Dolle P. Retinoic acid in development: towards an integrated view. Nat Rev Genet 2008;9:541–53.
3. Iwata M, Hirakiyama A, Eshima Y, Kagechika H, Kato C, Song SY. Retinoic acid imprints gut-homing specificity on T cells. Immunity 2004;21:527–38.
4. Svensson M, Johansson-Lindbom B, Zapata F, Jaensson E, Austenaa LM, Blomhoff R, et al. Retinoic acid receptor signaling levels and antigen dose regulate gut homing receptor expression on $CD8^+$ T cells. Mucosal Immunol 2008;1:38–48.
5. Eksteen B, Mora JR, Haughton EL, Henderson NC, Lee-Turner L, Villablanca EJ, et al. Gut homing receptors on CD8 T cells are retinoic acid dependent and not maintained by liver dendritic or stellate cells. Gastroenterology 2009;137:320–9.
6. Mora JR, Iwata M, Eksteen B, Song SY, Junt T, Senman B, et al. Generation of gut-homing IgA-secreting B cells by intestinal dendritic cells. Science 2006;314:1157–60.
7. Sun CM, Hall JA, Blank RB, Bouladoux N, Oukka M, Mora JR, et al. Small intestine lamina propria dendritic cells promote *de novo* generation of Foxp3 T reg cells via retinoic acid. J Exp Med 2007;204:1775–85.
8. Benson MJ, Pino-Lagos K, Rosemblatt M, Noelle RJ. All-trans retinoic acid mediates enhanced Treg cell growth, differentiation, and gut homing in the face of high levels of co-stimulation. J Exp Med 2007;204:1765–74.
9. Mucida D, Park Y, Kim G, Turovskaya O, Scott I, Kronenberg M, et al. Reciprocal TH17 and regulatory T cell differentiation mediated by retinoic acid. Science 2007;317:256–60.
10. Hall JA, Cannons JL, Grainger JR, Dos Santos LM, Hand TW, Naik S, et al. Essential role for retinoic acid in the promotion of CD4(+) T cell effector responses via retinoic acid receptor alpha. Immunity 2011;34:435–47.
11. Pino-Lagos K, Guo Y, Brown C, Alexander MP, Elgueta R, Bennett KA, et al. A retinoic acid-dependent checkpoint in the development of $CD4^+$ T cell-mediated immunity. J Exp Med 2011;208:1767–75.
12. Kusmartsev S, Cheng F, Yu B, Nefedova Y, Sotomayor E, Lush RM, et al. All-trans-retinoic acid eliminates immature myeloid cells from tumor-bearing mice and improves the effect of vaccination. Cancer Res 2003;63:4441–9.
13. Mirza N, Fishman M, Fricke I, Dunn M, Neuger AM, Frost TJ, et al. All-trans-retinoic acid improves differentiation of myeloid cells and immune response in cancer patients. Cancer Res 2006;66:9299–307.
14. Rosenberg SA, Yang JC, Restifo NP. Cancer immunotherapy: moving beyond current vaccines. Nat Med 2004;10:909–15.
15. Rajaii F, Bitzer ZT, Xu Q, Sockanathan S. Expression of the dominant negative retinoid receptor, RAR403, alters telencephalic progenitor proliferation, survival, and cell fate specification. Dev Biol 2008;316:371–82.
16. Wang L, Pino-Lagos K, de Vries VC, Guleria I, Sayegh MH, Noelle RJ. Programmed death 1 ligand signaling regulates the generation of adaptive $Foxp3^+CD4^+$ regulatory T cells. Proc Natl Acad Sci U S A 2008;105:9331–6.
17. Kane MA, Folias AE, Wang C, Napoli JL. Quantitative profiling of endogenous retinoic acid *in vivo* and *in vitro* by tandem mass spectrometry. Anal Chem 2008;80:1702–8.
18. Yokota A, Takeuchi H, Maeda N, Ohoka Y, Kato C, Song SY, et al. GM-CSF and IL-4 synergistically trigger dendritic cells to acquire retinoic acid-producing capacity. Int Immunol 2009;21:361–77.
19. Ahonen CL, Doxsee CL, McGurran SM, Riter TR, Wade WF, Barth RJ, et al. Combined TLR and CD40 triggering induces potent $CD8^+$ T cell expansion with variable dependence on type I IFN. J Exp Med 2004;199:775–84.
20. Turk MJ, Guevara-Patino JA, Rizzuto GA, Engelhorn ME, Sakaguchi S, Houghton AN. Concomitant tumor immunity to a poorly immunogenic melanoma is prevented by regulatory T cells. J Exp Med 2004;200:771–82.
21. Obar JJ, Khanna KM, Lefrancois L. Endogenous naive $CD8^+$ T cell precursor frequency regulates primary and memory responses to infection. Immunity 2008;28:859–69.
22. Guilliams M, Crozat K, Henri S, Tamoutounour S, Grenot P, Devilard E, et al. Skin-draining lymph nodes contain dermis-derived CD103(−) dendritic cells that constitutively produce retinoic acid and induce Foxp3(+) regulatory T cells. Blood 2010;115:1958–68.
23. Chambon P. A decade of molecular biology of retinoic acid receptors. FASEB J 1996;10:940–54.
24. Zhang P, Cote AL, de Vries VC, Usherwood EJ, Turk MJ. Induction of postsurgical tumor immunity and T-cell memory by a poorly immunogenic tumor. Cancer Res 2007;67:6468–76.
25. Engedal N, Ertesvag A, Blomhoff HK. Survival of activated human T lymphocytes is promoted by retinoic acid via induction of IL-2. Int Immunol 2004;16:443–53.
26. Ertesvag A, Austenaa LM, Carlsen H, Blomhoff R, Blomhoff HK. Retinoic acid inhibits *in vivo* interleukin-2 gene expression and T-cell activation in mice. Immunology 2009;126:514–22.